Supporting Information

ε-InSe single crystals grown by a Horizonal Gradient Freeze method

Maojun Sun,[ab] Wei Wang,[ab] Qinghua Zhao,[abc] Xuetao Gan,[e] Yuanhui Sun,[*d] Wanqi Jie,[ab] Tao Wang[* ab]

[a]State Key Laboratory of Solidification Processing, Northwestern Polytechnical University, Xi'an, 710072, P. R. China

[b]Key Laboratory of Radiation Detection Materials and Devices, Ministry of Industry and Information Technology, Northwestern Polytechnical University, Xi'an, 710072, P. R. China

[c]Materials Science Factory. Instituto de Ciencia de Materiales de Madrid (ICMM-CSIC), Madrid, E-28049, Spain

[d]Department of Chemistry and Biochemistry, California State University Northridge, Northridge, California, 91330, USA

[e]School of Physical Science and Technology, Northwestern Polytechnical University, Xi'an, 710072, P. R. China

[*]Corresponding Author:

yuanhui.sun@csun.edu (Yuanhui Sun); taowang@nwpu.edu.cn (Tao Wang)

Table of Content

Note 1: Theoretical prediction of formation energy of *γ*-InSe, *β*-InSe, *ε*-InSe

First-principles calculations were carried out within the framework of DFT by using plane-wave pseudopotential methods as implemented in the Vienna Ab initio Simulation Package.[1, 2] The electron-ion interactions were described by using the projected augmented wave pseudopotentials with $5s^2 5p^1$ (In) and $4s^2 4p^4$ (Se) treated as valence electrons.[3, 4] We used the generalized gradient approximation formulated by Perdew, Burke, and Ernzerhof as exchange-correlation functional.[5] A kinetic energy cutoff 500 eV was used for wave-function expansion, and the electronic intergration within the Brillouin zone was done with the k-point meshed of 15×15×1 and 15×15×9 for the multi-layer slabs and bulk materials, respectively. A vacuum layer of more than 20 Å thickness was used in layer-dependent calculations to isolate the InSe layer from its neighboring image. The structures (lattice parameters and atomic positions) were fully optimized including optB86b-vdW functional, until the residual forces were converged within 0.02 eV/Å.[6, 7]

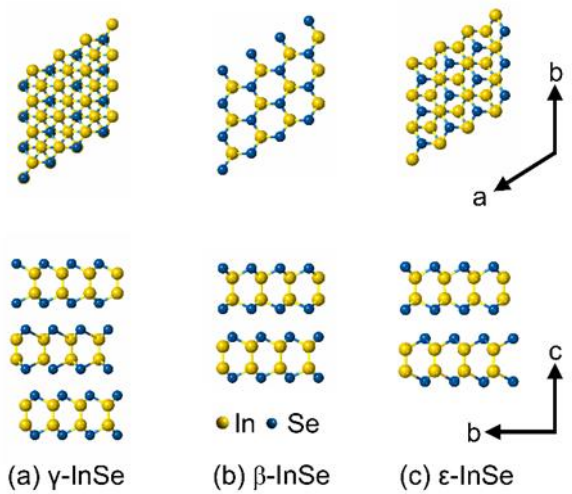

Fig. S1. Crystal structures of three bulk InSe phases:(a) γ-InSe. (b) β-InSe. (c) ε-InSe.

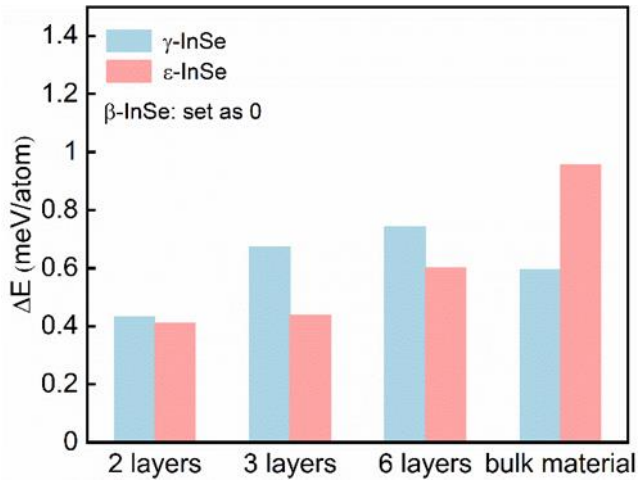

Fig. S2. Energy differences of InSe-based polymorphs under different layer thickness. The energy of β-InSe is set to zero.

Note 2: Growth of ε-InSe single crystals.

Synthesis of polycrystalline InSe. The InSe single crystals were grown by a Horizontal Gradient Freeze method (HGF). As shown in the Fig. 2a, two identical pBN boats

loading Se (6N) and In (6N) raw materials were placed in the two ends of a quartz tube. And after being evacuated (about 10^{-6} Torr) and sealed (by oxy-hydrogen flame), the quartz tube was placed into a tube furnace with multi-stage temperature controlling. Firstly, to ensure the Se source to be uniformly diffused, mixed and reacted with the In source by Physical Vapor Transport, the Se and In sources were heated at 1163 K and 963 K for 24 h, respectively.

Growth of single-crystalline InSe. Secondly, the InSe single crystal was acquired via Horizontal Gradient Freeze method. In addition, the growth parameters can be described as follows: growth temperature: 823-898 K; temperature gradient:3 K/cm; growth rate:1mm/h; cooling rate: 20 K/h.

Note 3: Experimental methods.

Characterization and identification and of *ε*-InSe. The SEM spectra were acquired via a Field Emission Scanning Electron Microscope (Zeiss Supra 55) equipped with a Energy Dispersive X-ray Spectroscopy (EDXS). The as-grown InSe crystals were ground into powder and collected X-ray Diffraction (XRD) pattern using a D/max2500 X-ray diffractometer with Cu-Kα radiation (λ=1.5406 Å). TEM measurements were conducted by using a transmission electron microscope (FEI Talos F200X), operated at an acceleration voltage of 100 kV in TEM mode and Selected area diffraction (SAED) mode. The photoluminescence (PL) spectrum was measured using a laser with the wavelength of 532 nm and the luminescence signals were recorded with the spectrometer of SpectraPro (Princeton, USA). The Raman spectrum was obtained by

using a inVia Raman microprobe (Renishaw) with spectral resolution of about 1 cm^{-1} equipped with a diode laser of a 532 nm. The IR adsorption spectrum was acquired via a Nicolet iS50 Fourier Transform Infrared Spectrometer (Thermo Fisher, USA). The few-layer InSe nanoflakes were cleaved from as-grown crystals and adhered to the 300 nm SiO_2 coated Si via mechanical exfoliation method. The thickness of the flakes was determined by optical image and atomic force microscope (AFM, Dimension FastScan and Dimension Icon system, Bruker, USA) under ambient conditions. The SHG measurements were carried out using a vertically coupled cross-polarization microscope, which has been introduced in another work.[8] A narrowband tunable telecom CW laser (Yenista, T100S-HP/CL) was employed as excitation light source. The frequency conversion signals scattered from the samples are collected by the objective lens (50X Mitutoyo 50Í), which pass through the short-pass dichroic mirror and are examined by a spectrometer (Princeton Instruments SP 2-500) equipped with a cooled silicon camera.

Note 4: TEM analysis of three InSe polytypes.

Because the TEM measurements were performed on the cleavage surface of the sample and the observed six-order symmetry of diffraction spots, the zone axis of the sample can be determined as [001]. Theoretically calculated electron diffraction patterns based on the three different crystal lattices were obtained using the CrystalMaker software. The crystal lattice parameters of monolayer InSe were set as a=b=4.01 Å and c=8.48 Å. As shown in Fig. S3, the nearest point distance from the center point for ε or β phase is

0.288 1/ Å. But for γ phase, the nearest point distance from the center point is 0.499 1/ Å. Therefore, we can absolutely conclude the γ phase.

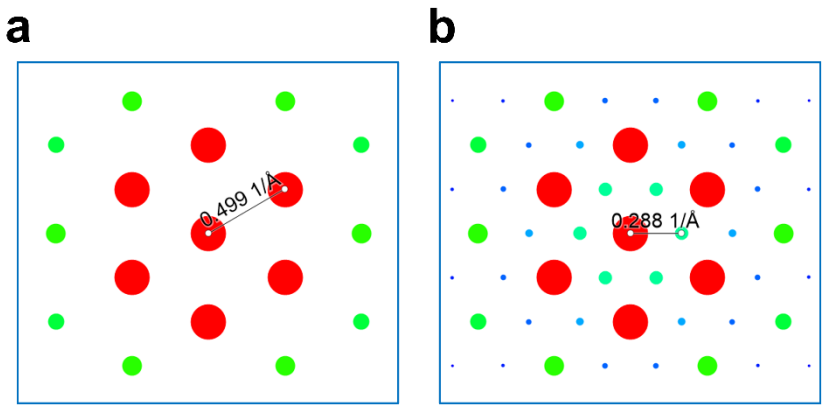

Fig. S3. Theoretically calculated electron diffraction pattern for three InSe phases: (a) γ-InSe, (b) ε-InSe or β-InSe.

To confirm the results, we further studied the possible planes for the three InSe phases. The distances of plane (hkl) were calculated using the formula (1) as follows and listed in Table S1.

$$d_{hkl} = \frac{a}{\sqrt{\frac{4}{3}\left(h^2 + hk + k^2\right) + \left(\frac{a}{c}\right)^2 l^2}} \quad (1)$$

Table S1. Possible planes for the nearest SAED points in the three phases

Polytypes	d_{hkl} (Å)	*hkl*	Intensity (%)
γ-InSe	8.480	(003)	59
	3.437	**(-111) & (101) & (0-11)**	100
	3.346	**(1-12) & (-102) & (012)**	72
	2.002	(110) & (2-10) & (-120)	90

	1.949	(2-13) & (-213) & (-123) & (1-23) & (-1-13) & (113)	8
ε-InSe	8.480	(002)	42
	3.468	**(-110) & (100) & (010)**	23
	3.398	**(-111) & (1-11) & (-101) & (0-11) & (011) & (101)**	100
	3.210	(1-12) & (-112) & (-102) & (102) & (0-12) & (012)	23
	2.956	(-113) & (1-13) & (103) & (-103) & (0-13) & (013)	60
	2.003	(2-10) & (-120) & (110)	72
	1.949	(-212) & (1-220 & (2-12) & (-122) & (112) & (-1-12)	6
β-InSe	8.480	(002)	49
	3.468	**(-110) & (100) & (010)**	100
	3.398	**(-111) & (101) & (1-11) & (-101) & (011) & (0-11)**	49
	3.210	(-112) & (-102) & (0-12) & (1-12) & (012) & (102)	8
	2.956	(0-13) & (-103) & (1-13) & (-113) & (013) & (103)	70
	2.003	(2-10) & (-120) & (110)	87
	1.949	(-122) & (-212) & (-1-12) & (1-22) & (2-12) & (112)	7

According to the SAED pattern image in Fig. 2, the possible plane distances are 3.468 Å, 3.437 Å, 3.398 Å or 3.346 Å. Thus, the possible zone axes for the three InSe phases can be found out and presented in Fig. S4. The only possible zone axis for *γ*-InSe is [211]. However, it is not likely to obtain such a pattern. There are two reasons listed as follows. First, the [211] deviates from [001] by 15.252° but the sample holder just can move up to 15° on each side. Secondly, the [211] is a four-fold axis while the measured SAED pattern seems like a six-fold one.

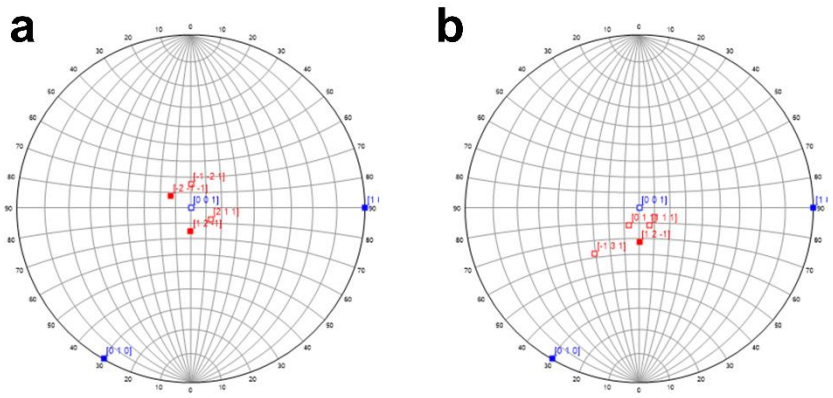

Fig. S4. Stereographic projection of all possible zone axes for the SAED pattern image of (a) γ-InSe, (b) ε-InSe or β-InSe.

References

1. G. Kresse and J. Furthmuller, *Computational Materials Science*, 1996, **6**, 15-50.
2. G. Kresse and J. Furthmuller, *Physical Review B*, 1996, **54**, 11169-11186.
3. P. E. Blochl, *Physical Review B*, 1994, **50**, 17953-17979.
4. G. Kresse and D. Joubert, *Physical Review B*, 1999, **59**, 1758-1775.
5. J. P. Perdew, K. Burke and M. Ernzerhof, *Physical Review Letters*, 1996, **77**, 3865-3868.
6. J. Klimes, D. R. Bowler and A. Michaelides, *Journal of Physics-Condensed Matter*, 2010, **22**, 022201.
7. J. Klimes, D. R. Bowler and A. Michaelides, *Physical Review B*, 2011, **83**, 195131.
8. X. T. Gan, C. Y. Zhao, S. Q. Hu, T. Wang, Y. Song, J. Li, Q. H. Zhao, W. Q. Jie and J. L. Zhao, *Light-Science & Applications*, 2018, **7**, 6.